Experimental detection of post-soliton structures following high intensity laser interaction with a sub-critical gas jet

G. Sarri[1], D. K. Singh[2], J. R. Davies[2], K. L. Lancaster[3], E. L. Clark[4], S. Hassan[4], J. Jiang[2], N. Kageiwa[5], N. Lopes[2], A. Rehman[6], C. Russo[2], R. H. H. Scott[3], T. Tanimoto[5], Z. Najmudin[6], K. A. Tanaka[6], M. Tatarakis[4], M. Borghesi[1], P. Norreys[3,6]

[1] *School of Mathematics and Physics, Queens University of Belfast, Belfast, UK*

[2] *GoLP, Instituto de Plasmas e Fusão Nuclear - Laboratório Associado, Instituto Superior Técnico, Lisbon, Portugal*

[3] *STFC Rutherford Appleton Laboratory, Didcot, UK*

[4] *Technological Educational Institute of Crete, Crete, Greece*

[5] *Graduate School of Engineering, Osaka, Japan*

[6] *Blackett Laboratory, Imperial College London, London, UK*

The creation of electromagnetic (e.m.) solitons [1, 2, 3, 4] during the interaction of a relativistically intense laser pulse ($a_0 \geq 1$) with a sub-critical ($n_c \geq n_e \geq 0.1n_c$) plasma is a phenomenon of great interest due to the predominant role that it plays during the laser energy dissipation [4]. Under proper conditions, up to 40% of the initial laser energy can be trapped in density depleted plasma cavities, whose radius is of the order of the electron collisionless skin depth. This is possible because, during its propagation, the laser experiences a frequency red-shift that eventually will make the surrounding plasma overcritical [5]. In the case of homogeneous plasmas, these cavities remain almost steady on the electron time scale whereas they start to radially expand on the ion time scale. This expansion is triggered by the Coulomb explosion of the positively charged soliton core. This late-time evolution of an e.m. soliton is commonly referred to as a *post-soliton* [6].

Despite the extensive theoretical work [6, 7], mostly based on the snowplow model [8] and the isolated spherical resonator model [9], experimental observations of post-soliton structures are limited to [10]. Here soliton remnants were observed in the dense region of a plasma resulting from the laser-driven explosion of a thin foil. Due to the nature of the plasma employed, clouds of bubble structures were detected thus preventing a precise characterisation of the temporal evolution of the post-solitons.

Here, we report the first experimental observation of well isolated post-soliton structures. This allows their evolution to be resolved and followed over a significant temporal window. The experimental results are compared to analytical and three dimensional (3D) Particle-In-Cell (PIC) code models.

The experiment was carried out at the Rutherford Appleton Laboratory employing the VUL-

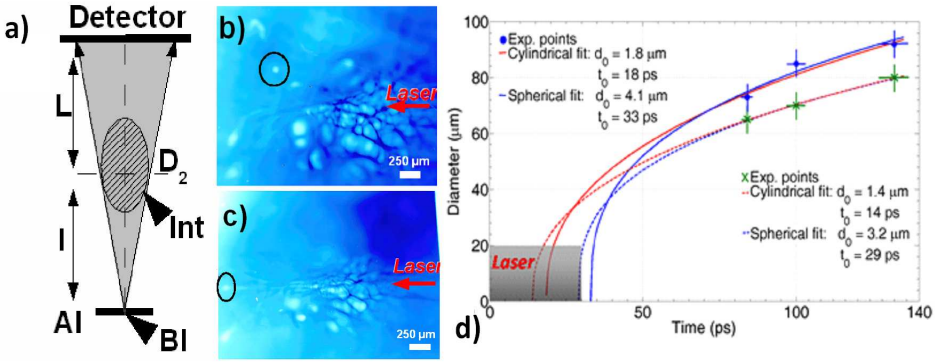

Figure 1: **a)** Top view of the experimental arrangement. **b), c)** Radiographs of two different shots: outlined with dark circles are the density bubbles interpreted to be post-solitons.**d)** Bubble diameter as a function of time and fits using results from the snowplow model for cylindrical and spherical post-solitons.

CAN Nd:glass laser [11]. A sketch of the set up is given in Fig.1: 200 J of 1 μm laser light contained in a 30 ps Full Width Half Maximum pulse ("Int" in Fig. 1) were focussed to a peak intensity of 3×10^{18} W cm^{-2} at the edge of a supersonic deuterium gas jet with a backing pressure ranging from 1 to 100 bar. This resulted, once fully ionized, in an electron density of 10^{18}–10^{20} cm^{-3}, which is 0.001–0.1 times the non-relativistic critical density n_c. The interaction was diagnosed via the proton radiography technique [10, 12], which uses, as a particle probe, a laser accelerated proton beam, arising from the interaction of a secondary laser pulse ($\tau \approx 1$ ps, $E \approx 100$ J, $I \geq 10^{19}$ W cm^{-2}, "Bl" in Fig. 1) with a 20μm thick aluminium foil. The beam, after having passed through the gas jet, was recorded by a stack of RadioChromic Films (RCF) [13].

The data set comprised about 30 shots in which both the deuterium density and the probe time were varied. Bubble-like structures, that we ascribe here to post-solitons, were ever obtained only at densities of $0.1n_c$. Two typical images obtained at this regime are shown in Fig. 1; these images were obtained with protons of energy ≈ 4 MeV, 100 ps after the beginning of the interaction. In both images a strongly modulated deflection pattern is visible along the laser propagation axis. This scaly region highlights the presence of a cloud of bubbles that look to be merged or overlying one another in this 2D projection, possibly surrounding the laser-driven channel. Such a region visually resembles the cloud of solitons reported in [10]. Ahead of and around this region, isolated bubble-like structures are visible (black circles in Fig. 1), most of them located at the tip of the laser filaments, as numerically predicted in [2]. Considering the

isolated bubbles allows following the fundamental properties of the post-soliton temporal evolution and we will thus restrict the discussion just to those.

The multi-frame capability of proton radiography [12] allowed following the temporal evolution of these bubbles in the range 80–130 ps after the beginning of the interaction. Both bubbles analysed were found to be effectively stationary in the laboratory reference frame and to radially expand (Fig.1.d). Their expansion was fitted with the analytical scalings, derived in the framework of the snowplow model, obtained in [7] for 2D cylindrical and 3D spherical post-solitons; the initial soliton diameter d_0 and the creation moment t_0 were kept as free parameters. It has to be noted here that a good fit should give d_0 of the order of two times the electron skin depth and t_0 close to the peak of the laser pulse.

Even though the spherical scaling was able to fit the experimental data, it implied a creation time at the end of, if not after, the laser pulse duration and a too large initial soliton diameter (see Fig. 1.d); both these results are not physically sensible. We therefore tried the 2D cylindrical result: this gave a more physically meaningful fit with a creation time close to the peak of the laser pulse and an initial diameter of the order of the electron skin depth (see Fig. 1.d).

In order to understand why a 3D structure follows predictions for 2 rather than 3 dimensions,

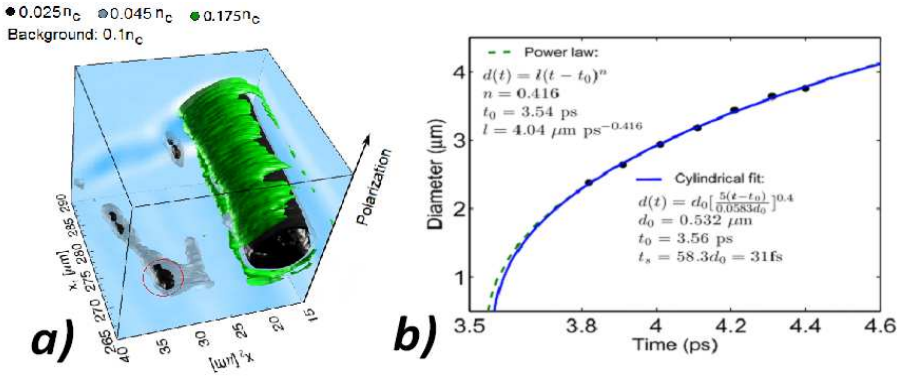

Figure 2: **a)**Iso-surfaces of the ion density at 4.11 ps from 3D PIC modeling. **b)**Post-soliton diameter X_2 extracted from the 3D PIC results along with a power law fit and a fit using the analytical result for a cylindrical post-soliton.

we carried out a 3D run with the PIC code OSIRIS [14]. We considered a linearly polarized laser pulse with a wavelength of 1 μm, Gaussian spatial and temporal profiles with FWHM of 6 μm and 1 ps, respectively, and a peak intensity of 3×10^{18} W cm^{-2} incident on a fully ionized deuterium plasma with a density of $0.1n_c$. The interaction was followed for 5 ps. The simulation box was $350 \times 50 \times 50$ μm, divided into 2.4×10^8 cells each having 2 particles for electrons and 2 for deuterium ions, the time step was 0.196 fs. The ion density in Fig. 2 shows

prolate spheroid post-solitons, elongated along the laser propagation axis, as also obtained in [3]. These structures are lying outside the channel formed by the laser, in the plane perpendicular to the laser electric field. The expansion of the simulated bubbles follows a cylindrical expansion too (see Fig. 2.b). The anisotropic expansion of the post-soliton might be due to polarization effects, consistently with [2]. The snowplow model, which predicts purely spherical expansions, assumes in fact total reflection of the trapped light at the overcritical soliton wall and therefore no plasma heating. This is a good approximation only for *s*-polarized light, since a *p*-polarized wave will be significantly absorbed by the overcritical walls. This might explain why *p*-polarized light is not able to excite stable e.m. solitons [2].

References

[1] D. Farina and S. V. Bulanov, Phys. Rev. Lett., **86**,5289 (2001).

[2] S. V. Bulanov *et al.*, Phys. Rev. Lett., **82**,3440 (1999).

[3] T. Esirkepov *et al.*, Phys. Rev. Lett., **89**,275002 (2002)

[4] G. Lehmann *et al.*, Phys. Plasmas, **13**,092302 (2006).

[5] S. V. Bulanov *et al.*, Phys. Fluids B, **4**,1935 (1992).

[6] N. M. Naumova *et al.*, Phys. Rev. Lett., **87**,185004 (2001).

[7] S. V. Bulanov and F. Pegoraro, Phys. Rev. E, **65**,066405 (2002).

[8] Ya. B. Zel'dovich and Yu. P. Raizer, *Physics of Shock Waves and High-Temperature Hydrodynamic Phenomena* (Academic Press, New York, 1967).

[9] L. D. Landau and L. M. Lifshits, *Electrodynamics of continuous media* (Pergamon, Oxford, 1984)..

[10] M. Borghesi *et al.*, Phys. Rev. Lett., **88**,135002 (2002).

[11] C. Hernandez-Gomez *et al.* RAL report no. RAL-TR-2008-025, p. 260, ISBN 978-0-9556616-4-8 (2008).

[12] G. Sarri *et al.*, New J. Phys. **12**,045006 (2010).

[13] J.F.Dempsey *et al.* Med. Phys. **27**,10 (2000).

[14] R.A. Fonseca, L.O. Silva, R.G. Hemker, Lect. Not. Comp. Sci. **2331**,342 (2002).